Forschungszentrum Karlsruhe
in der Helmholtz-Gemeinschaft
Wissenschaftliche Berichte
FZKA 7451

Deformation and Lifetime Prediction Model for RAFM Steels under Creep-Fatigue and High Dose Irradiation Conditions

Final Report
TW2-TTMS-005b, D4
(Modeling part)

J. Aktaa, C. Petersen

Institut für Materialforschung
Programm Kernfusion
Association Forschungszentrum Kalrsruhe/EURATOM

Dezember 2009

Forschungszentrum Karlsruhe

in der Helmholtz-Gemeinschaft

scientific reports

FZKA 7451

Deformation and lifetime prediction model for RAFM steels under creep-fatigue and high dose irradiation conditions

Final Report:

TW2-TTMS-005b, D4

(Modeling part)

J. Aktaa and C. Petersen

Institut für Materialforschung

Programm Kernfusion

Association Forschungszentrum Karlsruhe/EURATOM

Forschungszentrum Karlsruhe GmbH, Karlsruhe

2010

Forschungszentrum Karlsruhe GmbH
Postfach 3640, 76021 Karlsruhe

Mitglied der Hermann von Helmholtz-Gemeinschaft
Deutscher Forschungszentren (HGF)

ISSN 0947-8620

urn:nbn:de:0005-074512

Report for TASK of the EFDA Technology Programme			
Reference:	Field: Tritium Breeding and Materials Area: Materials Development Task: TW2-TTMS-005b Task Title: Rules for Design Fabrication and Inspection Subtask Title: Evaluation of lifetime rules under irradiation creep and creep-fatigue and high fluence conditions. Proposal and implementation of rules. Development of verification experiments. Deliverable No.: D4		
Document:	Deformation and lifetime prediction model for RAFM steels under creep-fatigue and high dose irradiation conditions		
Level of confidentiality	Free distribution ☒ Confidential ☐ Restricted distribution ☐		
Author(s):	J. Aktaa and C. Petersen Forschungszentrum Karlsruhe, Germany		
Date:	29 January 2010		
Distribution list:	Rainer Laesser (Field Co-ordinator) Eberhard Diegele (Responsible Officer) Bob van der Schaaf (Project Leader) Farhad Tavassoli (Task Co-ordinator)		
Abstract:	A viscoplastic deformation damage model developed for RAFM steels in the reference un-irradiated state was modified taking into account the irradiation influence. The modification mainly consisted in adding an irradiation hardening variable with an appropriate evolution equation including irradiation dose driven terms as well as inelastic deformation and thermal recovery terms. With this approach, the majority of the material and temperature dependent model parameters are no longer dependent on the irradiation dose and only few parameters need to be determined by applying the model to RAFM steels in the irradiated state. The modified model is applied to describe the behavior of the RAFM steels, EUROFER 97 and F82H mod, observed in post irradiation examinations among others of the irradiation programs ARBOR 1 and ARBOR 2. Thereby tensile and low cycle fatigue tests are considered determining the material and temperature dependent parameters of the model and verifying its prediction capability.		
Revision No: -	Changes: -		
	Written by:	Revised by:	Approved by:
	Jarir Aktaa	Mario Walter	Oliver Kraft

Verformungs- und Lebensdauervorhersagemodel für RAFM-Stähle unter Kriech-Ermüdungs- und Hochdosisbestrahlungsbedingungen

Zusammenfassung

Das zur Beschreibung des Verhaltens von RAFM-Stählen im unbestrahlten Referenzzustand entwickelte viskoplastische Verformungs-Schädigungsmodel wurde modifiziert, um auch den Bestrahlungseinfluss zu berücksichtigen. Die Modifikation bestand hauptsächlich aus der Einführung einer Variablen für die bestrahlungsinduzierte Verfestigung mit einer geeigneten Entwicklungsgleichung. Die Gleichung enthält zum einen von der Bestrahlungsdosis gesteuerten Terme und zum anderen solche, die die durch die inelastische Verformung und thermische Auslagerung verursachte Erholung beschreiben. Bei diesem Ansatz sind die meisten material- und temperaturabhängigen Modellparameter unabhängig von der Bestrahlungsdosis, so dass nur wenige Parameter für die Anwendung auf RAFM-Stähle im bestrahlten Zustand zu bestimmen sind. Das modifizierte Modell wurde angewendet, um das Verhalten der RAFM-Stähle, EUROFER 97 and F82H mod, zu beschreiben, wie es in den Nachbestrahlungsuntersuchungen unter anderem der Bestrahlungsprogramme ARBOR 1 und ARBOR 2 beobachtet wurde. Für die Bestimmung der material- und temperatur-abhängigen Modellparameter und die Verifikation der Modellvorhersage wurden Zug- und Kurzzeitermüdungsversuche betrachtet.

Abstract

A viscoplastic deformation damage model developed for RAFM steels in the reference un-irradiated state was modified taking into account the irradiation influence. The modification mainly consisted in adding an irradiation hardening variable with an appropriate evolution equation including irradiation dose driven terms as well as inelastic deformation and thermal recovery terms. With this approach, the majority of the material and temperature dependent model parameters are no longer dependent on the irradiation dose and only few parameters need to be determined by applying the model to RAFM steels in the irradiated state. The modified model is applied to describe the behavior of the RAFM steels, EUROFER 97 and F82H mod, observed in post irradiation examinations among others of the irradiation programs ARBOR 1 and ARBOR 2. Thereby tensile and low cycle fatigue tests are considered determining the material and temperature dependent parameters of the model and verifying its prediction capability.

TABLE OF CONTENTS

1 Introduction

Reduced activation ferritic martensitic (RAFM) steels, among others EUROFER 97 and F82H, are promising candidates as structure materials for first wall components of future fusion power plants [1, 2]. During an operation period of 2 years, the structure material shall be subjected to an irradiation dose of up to 100 dpa (displacements per atom) yielding remarkable irradiation induced embrittlement and changes in its mechanical behavior [3, 4]. Considering these changes correctly in the design assessment procedure of the components is a precondition for a reliable operation. Therefore constitutive models describing the deformation and damage behavior of RAFM steels in the irradiated state under operation loadings are required.

In our approach, we started developing a deformation damage model describing the behavior of RAFM steels in the un-irradiated state [5]. The model accounts for many characteristics originating from the unique microstructure of these materials, among others the non-linear strengthening behavior under monotonic loading, complex non-saturating softening under cyclic loading and material deterioration under creep-fatigue loading [5]. Within the work reported here, the model was then modified to take irradiation into consideration by modeling the irradiation induced hardening and its interaction with the deformation and damage behavior. The resulting irradiation hardening model comprises the hardening induced by neutron irradiation as well as its alteration due to inelastic deformation and its recovery at high temperatures. All these phenomena are observed in post irradiation examinations on RAFM steels. However the applicability of the irradiation hardening model developed is not restricted to RAFM steels and it can be extended to other materials showing at least qualitatively similar behavior.

Irradiation induced hardening physically is a result of numerous irradiation damage mechanisms which will be reviewed briefly below. They are the basis of the irradiation hardening model developed which will be illustrated later on. Afterwards application of the model to EUROFER 97 will be presented and discussed.

2 Irradiation damage mechanisms

Kinetic energy exchanges between energetic neutrons and atoms or between knocked-on atoms and other atoms in the lattice create both simple lattice defects, such as interstitial atoms and vacancies, and complex defects, such as displacement spikes [6]. Simple lattice defects can combine to form vacancy clusters which might reach a critical size and collapse to form stacking faults bounded by dislocation loops [7]. Displacement spikes consist of void regions containing vacancy clusters and some highly strained regions containing interstitials. In addition to lattice defects originating from atomic displacement neutrons are captured by atomic nuclei which subsequently transmute to new elements and possible co-product, such as helium or other noble gases [8]. Since these gases are highly insoluble in the lattice they interact with vacancies and form gas bubbles.

Vacancy clusters, dislocation loops, displacement spikes and helium gas bubbles can be considered as obstacles of different types which impede dislocation motion, increase strength and reduce ductility. They all can be formed in RAFM steels during neutron irradiation causing the so-called irradiation induced hardening. Hereinafter, they will just be referred to as obstacles of different types.

3 Modeling of irradiation induced hardening

The theory of the cutting of an obstacle by a dislocation line suggest that the resulting hardening σ_H should be proportional to the square root of the obstacle's volume density N provided that the mean obstacle diameter remains constant. Since we may have n_H different types of obstacles where each type i has its specific volume density N_i and causes a specific amount of hardening $\sigma_{H,i}$ the overall hardening results in

$$\sigma_H = \sum_{i=1}^{n_H} \sigma_{H,i} \qquad with \quad \sigma_{H,i} = h_i \sqrt{N_i} \tag{1}$$

N_i is expected to be initially proportional to the neutron dose ϕ but as the dose increases a saturation effect may occur which limits the obstacle volume density to $N_{s,i}$ [9]. Accordingly, for the evolution of N_i the following can be written:

$$\dot{N}_i = a_i (N_{s,i} - N_i)\, \dot{\phi} \tag{2}$$

h_i, a_i and $N_{s,i}$ are temperature and material dependent parameters. While h_i reflects how strong the dislocation pileup by the obstacle type i is, a_i is directly related to the formation rate of this obstacle type with respect to irradiation dose, and $N_{s,i}$ gives the maximum volume density can be obtained for this obstacle type achieving a balance between initiation and annihilation. Hence, these parameters are strongly influenced by the material specific microstructure. Assuming that they are known the irradiation induced hardening and the respective increase of yield stress can be determined using the equations above.

However, inelastic deformation and lattice slip activities, respectively, are expected to resolve irradiation defects at least within the associated slip bands [10], such that the volume density of certain obstacle types decreases while the material deforms inelastically. On the other hand, since irradiation induced defects would restrict largely the number of active slip bands the inelastic deformation can be localized microscopically by the forming of channels. Healing of irradiation induced defects is expected to be limited and to be highest in the channel band. To describe the resulting change in N_i as an average over the volume of the representative volume element - whose behavior is in fact modeled here -, the following modification of eq. (2) is proposed:

$$\dot{N}_i = a_i (N_{s,i} - N_i)\,\dot{\phi} - b_i (N_i - N_{l,i})\,\dot{p} \qquad (3)$$

$\dot{p}$ is the uniaxial equivalent inelastic strain rate which can also be interpreted as a volume average for the inelastic deformations possibly localized in channels within the representative volume element. $N_{l,i}$ gives the volume density of the irradiation induced obstacles remaining after a sufficiently large amount of inelastic deformation. Assuming that a sufficiently large amount of inelastic deformation would remove always the same amount of irradiation induced hardening $N_{l,i}$ can be determined as:

$$N_{l,i} = \left\langle \sqrt{\max_{-\infty<\tau<t} N_i(\tau)} - \sqrt{N_{r,i}} \right\rangle^2 \qquad (4)$$

b_i and $N_{r,i}$ are additional temperature and material dependent parameters. b_i is directly related to the healing rate of the obstacle type i with respect to inelastic deformation and $N_{r,i}$ represents the amount of this obstacle type which is formed at sufficiently high irradiation dose and can not be resolved by inelastic deformation. The brackets $\langle\ \rangle$ operate on the term in between as follows: $\langle x \rangle = (x + |x|)/2$. At a sufficiently high temperature diffusion processes may contribute to the healing of irradiation induced defects and, thus, to static recovery of irradiation induced hardening. This can be described by adding a static recovery term in eq. (3) resulting in

$$\dot{N}_i = a_i (N_{s,i} - N_i)\,\dot{\phi} - b_i (N_i - N_{l,i})\,\dot{p} - r_i N_i^{q_i} \qquad (5)$$

with r_i and q_i denoting further temperature and material dependent parameters. Irradiation induced hardening σ_H, the evolution of which can now be calculated using eqs. (1) and (5) even under inelastic deformation and high temperature dwell conditions, is assumed to influence the deformation and damage behavior like isotropic hardening by increasing the size of the inelastic yield surface in stress space. Accordingly the deformation damage model already developed for RAFM steels in the reference un-irradiated state under low cycle fatigue conditions [5] is simply modified to cover irradiation effects by incorporating σ_H in the flow rule for inelastic deformation as follows (refer to [5]):

$$\dot{\varepsilon}^{in} = \left\langle \frac{|\Sigma| - \sigma_H - k}{Z} \right\rangle^n \operatorname{sgn}(\Sigma) \quad \text{with} \quad \Sigma = \frac{\sigma}{\psi(1-\mathrm{D})} - \Omega \qquad (6)$$

$\dot{\varepsilon}^{in}$ and σ denote the inelastic strain rate and the applied stress, respectively. Ω, ψ and D are internal state variables describing the kinematic hardening, the isotropic softening and the damage, respectively. k, Z and n are temperature and material dependent parameters whereas k is equal to the initial yield stress and, thus, determines the initial size of the inelastic yield surface.

Incorporating σ_H in the flow rule for inelastic deformation by Eq. (6) allows the coupling between the irradiation induced hardening model introduced above and the deformation damage model developed to describe the behavior of RAFM steels in the reference un-irradiated state under arbitrary thermo-mechanical low cycle fatigue loadings [5, 11]. This coupling results in an overall model for predicting the deformation and lifetime behavior of RAFM steels under arbitrary loading and irradiation conditions. In the following a brief description of the coupled model is given and thereafter the results of its application to the RAFM steels EUROFER 97 and F82H mod are presented and discussed.

4 Deformation damage model for RAFM steels under irradiation

Within the continuum approach adopted for describing the coupled viscoplastic deformation damage behavior the total strain rate $\dot{\varepsilon}$ is subdivided in an elastic $\dot{\varepsilon}^{el}$, an inelastic $\dot{\varepsilon}^{in}$ and a thermal part $\dot{\varepsilon}^{th}$:

$$\dot{\varepsilon} = \dot{\varepsilon}^{el} + \dot{\varepsilon}^{in} + \dot{\varepsilon}^{th} \qquad \text{with} \qquad \varepsilon^{th} = \alpha \ (\mathrm{T} - \mathrm{T}_0) \ , \qquad \varepsilon^{el} = \frac{\sigma}{E\,(1-\mathrm{D})} \tag{7}$$

While in Eq. (1) the elastic and the thermal strain are determined by the Hook's and the thermal expansion law, respectively, the evolution of the inelastic strain is given by the following flow rule:

$$\dot{\varepsilon}^{in} = \left\langle \frac{|\Sigma| - \sigma_H - k}{Z} \right\rangle^n \mathrm{sgn}(\Sigma) \qquad \text{with} \qquad \Sigma = \frac{\sigma}{\psi(1\text{-}\mathrm{D})} - \Omega \tag{8}$$

Z, n and k are like the Young modulus E and the thermal expansion α material and temperature dependent parameters. σ denotes the applied stress and Ω, ψ, σ_H and D are internal variables for the kinematic hardening, isotropic softening, irradiation induced hardening and damage, respectively. It should be noticed that damage influences the elastic and inelastic deformation (see Eq. 7 and Eq. 8) according the effective stress concept of the continuum damage mechanics. For the internal variables evolution equations are proposed which reflects their dependence on the loading history:

Kinematic hardening

$$\dot{\Omega} = H\,\dot{\varepsilon}^{in} - Q\,\Omega\left|\dot{\varepsilon}^{in}\right| - R\left|\Omega\right|^{m-1}\Omega + \frac{1}{H}\frac{\partial H}{\partial T}\Omega\dot{T} \tag{9}$$

Isotropic softening

$$\psi = \psi_1 + \psi_2 \qquad \text{with} \qquad \psi_1\,(\mathrm{t}=0) = 0 \quad , \quad \psi_2\,(\mathrm{t}=0) = 1 \qquad \text{and}$$

$$\dot{\psi}_1 = -h\,\left|\dot{\varepsilon}^{in}\right|$$

$$\dot{\psi}_2 = c\ (\psi_s - \psi_2)\left|\dot{\varepsilon}^{in}\right| - r_\psi \left|\psi_2 - \psi_r\right|^{m_\psi - 1}(\psi_2 - \psi_r)$$

$$\text{with} \qquad \psi_s = 1 - \psi_{s,\infty}\left(1 - \exp\left(-c_s \max_{-\infty<\tau<t}\left|\varepsilon^{in}(\tau)\right|\right)\right) \tag{10}$$

Irradiation induced hardening

$$\sigma_H = \sum_i^{n_H} \sigma_{H,i} \qquad \text{with} \qquad \sigma_{H,i} = \sqrt{X_i} \quad \text{and}$$

$$\dot{X}_i = a_i\left(X_{s,i} - X_i\right)\dot{\phi} - b_i\left(X_i - X_{l,i}\right)\left|\dot{\varepsilon}^{in}\right| - r_{X,i} X^{q_{X,i}}$$

$$\text{with} \qquad X_{l,i} = \left\langle \sqrt{\max_{-\infty<\tau<t}\left|X_i(\tau)\right|} - \sqrt{X_{r,i}} \right\rangle^2 \tag{11}$$

$$X_{s,i} = h_i^2 N_{s,i}\ ,\ X_{r,i} = h_i^2 N_{r,i}\ ,\ r_{X,i} = r_i\ h_i^{2(1-q_i)}\ ,\ q_{X,i} = q_i$$

Damage

$$\dot{D} = \left\langle \frac{\sigma}{A} \right\rangle^r \left|\dot{\varepsilon}^{in}\right| \ (1 - D)^{-\kappa} \tag{12}$$

ϕ denotes the irradiation dose quantified in dpa (displacement per atom). H, Q, R, m, h, c, r_ψ, ψ_r, m_ψ, $\psi_{s,\infty}$, c_s, a_i, $X_{s,i}$, b_i, $X_{r,i}$, $r_{X,i}$, $q_{X,i}$, A, r and κ are additional material and temperature dependent parameters and can be determined by fitting the model response to the material behavior observed experimentally using suitable strategies [5, 11].

The influence of irradiation is considered by the model with the irradiation induced hardening variable σ_H which affects the inelastic deformation behavior (see Eq. 8) and thus the damage evolution indirectly. However, no change in the mechanism and evolution equation of damage due to irradiation is assumed.

The model above takes into account all first order deformation and damage phenomena as they observed in mechanical characterization experiments on RAFM steels in the un-irradiated and the irradiated state as well. Its formulation allows the implementation in commercial finite element codes and thus best prediction of the mechanical performance and reliability of components under fusion reactor conditions.

5 Application of the model to RAFM steels

5.1 Identification of model parameters

A precondition for the application of the model above is that sufficient data are available for the determination of the model parameters. In former applications on the RAFM steels EUROFERE 97 and F82H mod the major parts of the parameters, particularly those relevant for describing the material behavior in the un-irradiated state, were identified for different temperatures [5].

To determine the parameters of the model part describing irradiation induced hardening (eq. 11) the data available so far for EUROFER 97 and F82H mod from the literature and ongoing irradiation programs are considered which are anyhow limited and hence, the parameters can be determined for these two materials at certain temperatures. We started to use the model to describe the increase in yield stress determined after irradiation in post irradiation tensile testing. For this purpose, literature data [12, 13] as well as the data determined recently within the irradiation programs SPICE and ARBOR 1 and 2 were considered. Assuming that hardening is induced by only one type of obstacles (n_H in eq. (11) is equals 1), the model yields the following dependence of σ_H and yield stress increase, respectively, on the irradiation dose ϕ:

$$\sigma_H = h\sqrt{N_s}\left(1-\exp(-a\phi)\right)^{0.5} \qquad (7)$$

Fitting this relation to the experimental values of $\sigma_{H,0.2}$ (σ_H at 0.2% inelastic deformation), a fairly good description is obtained with $a = 0.132\,\mathrm{dpa}^{-1}$ and $h\sqrt{N_s} = 523.5\,\mathrm{MPa}$ for EUROFER 97 and with $a = 0.133\,\mathrm{dpa}^{-1}$ and $h\sqrt{N_s} = 480.57\,\mathrm{MPa}$ for F82H mod (see Figure 1). It should be noticed that the parameters a and N_s depend on the irradiation temperature only, while the parameter h reflects the dependence of σ_H on the temperature at which it is determined (test temperature). For the data considered the test temperature (300°C) is approximately equals the irradiation temperature.

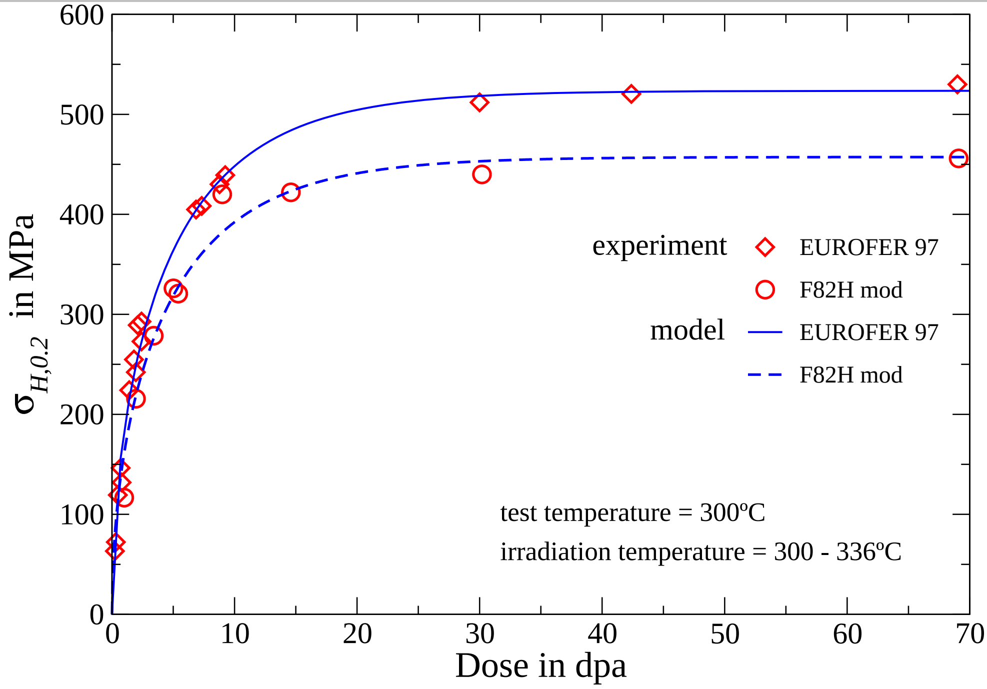

Figure 1 Irradiation induced hardening as a function on irradiation dose, comparison between experimental data (markers) and model description (solid line) [14, 15].

To describe the changes of σ_H within the course of inelastic deformation the stress – inelastic strain curves measured in tensile tests on the irradiated material with different doses are compared with the curve obtained for the material in the reference un-irradiated state at the same temperature (300 – 350°C). By subtraction in the small strain range (< 5%) the decrease of σ_H with increasing inelastic deformation can be determined starting from its initial value after irradiation and 0.2% inelastic deformation $\sigma_{H,0.2}$ (see Figure 2 and Figure 3 for EUROFER 97 and F82H mod, respectively). For the value of σ_H after a certain amount of accumulated inelastic deformation p, the following relation can be derived from the model (eqs. (1) and (5)) by neglecting static recovery:

$$\sigma_H = \left[\left(\sigma_{H,0.2} - \sigma_r\right)^2 + \left(\sigma_{H,0.2}^2 - \left(\sigma_{H,0.2} - \sigma_r\right)^2\right)\exp\left(-b\left(p - 0.002\right)\right)\right]^{0.5} \qquad (8)$$

Also this relation delivers a fairly good description of the experimental data with $b = 78.5$ and $\sigma_r = h\sqrt{N_r} = 298.6\,\mathrm{MPa}$ for EUROFER 97 and with $b = 73.725$ and $\sigma_r = 212.23\,\mathrm{MPa}$ for F82H mod (see Figure 2).

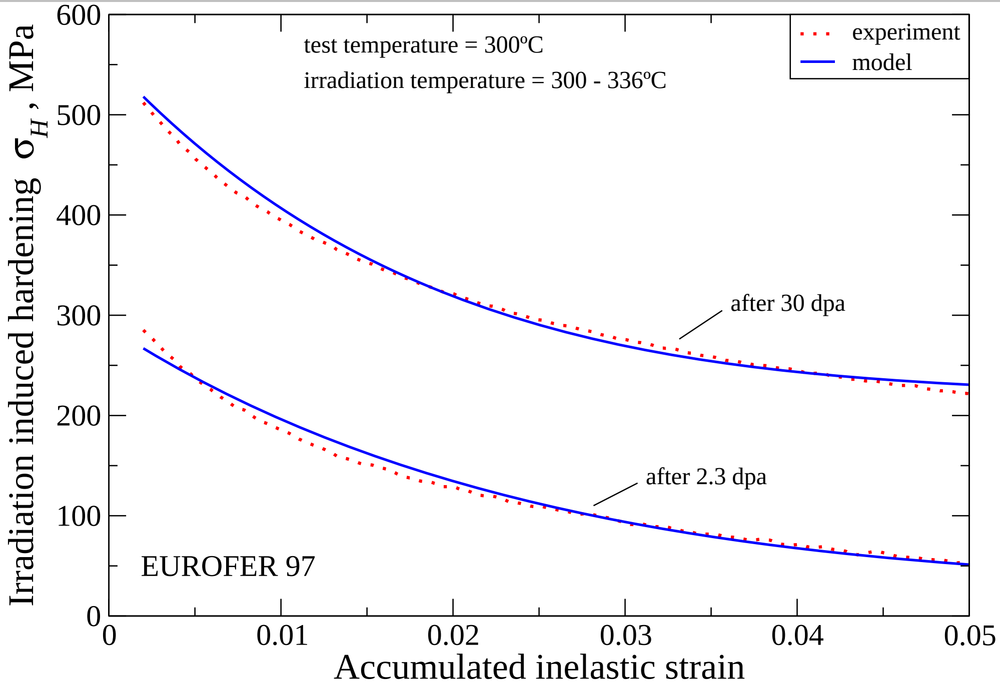

Figure 2: Influence of inelastic deformation on irradiation induced hardening of EUROFER 97; comparison between experimental data (doted lines) and model description (solid lines) [14].

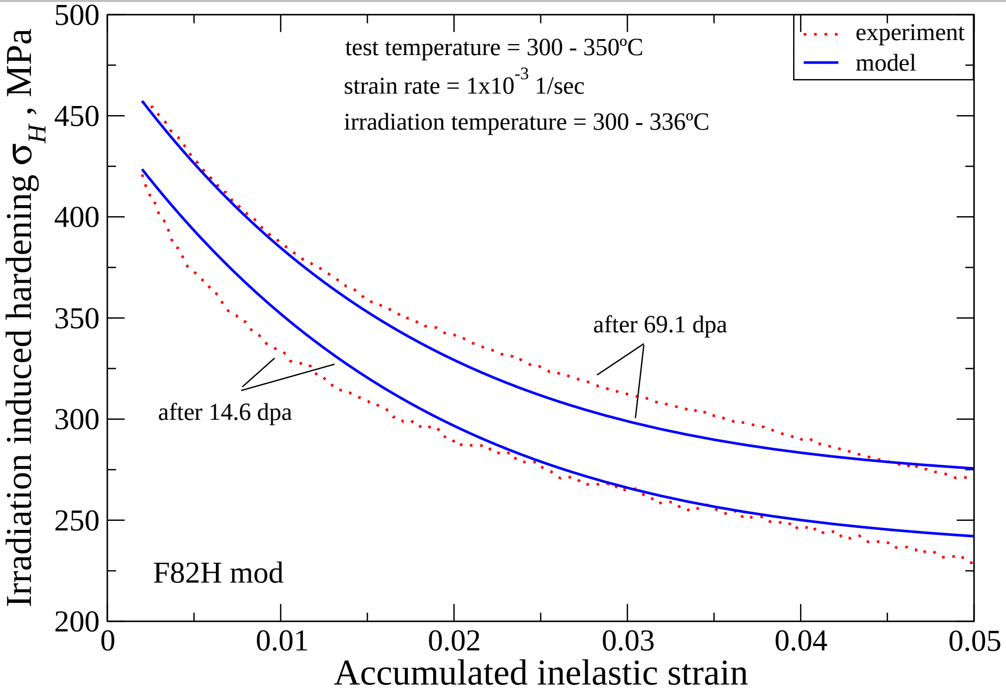

Figure 3: Influence of inelastic deformation on irradiation induced hardening of F82H mod; comparison between experimental data (doted lines) and model description (solid lines) [15].

Since the temperatures within 300 - 350°C are particularly for static recovery too low the remaining parameters of the model r and q can be assumed equal to 0 at these temperatures. For higher temperatures, however, these two parameters can be determined best by performing annealing heat treatments on irradiated specimens at the respective temperature with different durations and measuring afterwards the resulting decrease of the yield stress and the irradiation induced hardening, respectively. When applying the model (eqs. (1) and (5)) the dependence of $\sigma_{H,0.2}$ on the annealing duration t reads

$$\sigma_{H,0.2} = \left[-r*(1-q)\,t + \left(\sigma^0_{H,0.2}\right)^{2(1-q)}\right]^{0.5/(1-q)} \qquad (9)$$

with $r* = r\,h^{2(1-q)}$ and $\sigma^0_{H,0.2}$ being the value of $\sigma_{H,0.2}$ before the annealing heat treatment. Within ARBOR 2 irradiation program such annealing experiments are conducted on EUROFER 97 tensile specimens irradiated with a dose of 69 dpa at 332°C. The specimens are annealed at 550°C for 1 and 3 hours, respectively, and subsequently tested at 350°C. From the measured tensile curves the values of $\sigma_{H,0.2}$ are extracted and plotted versus the annealing duration in Figure 4. Fitting of eq. 9 to these values results in a fairly good description (s. Figure 4), with $r* = 5.707 \times 10^{-5}\ \mathrm{MPa}^{2(1-q)}/\mathrm{sec}$ and $q = 1.288$ representing the values of these parameters at 550°C.

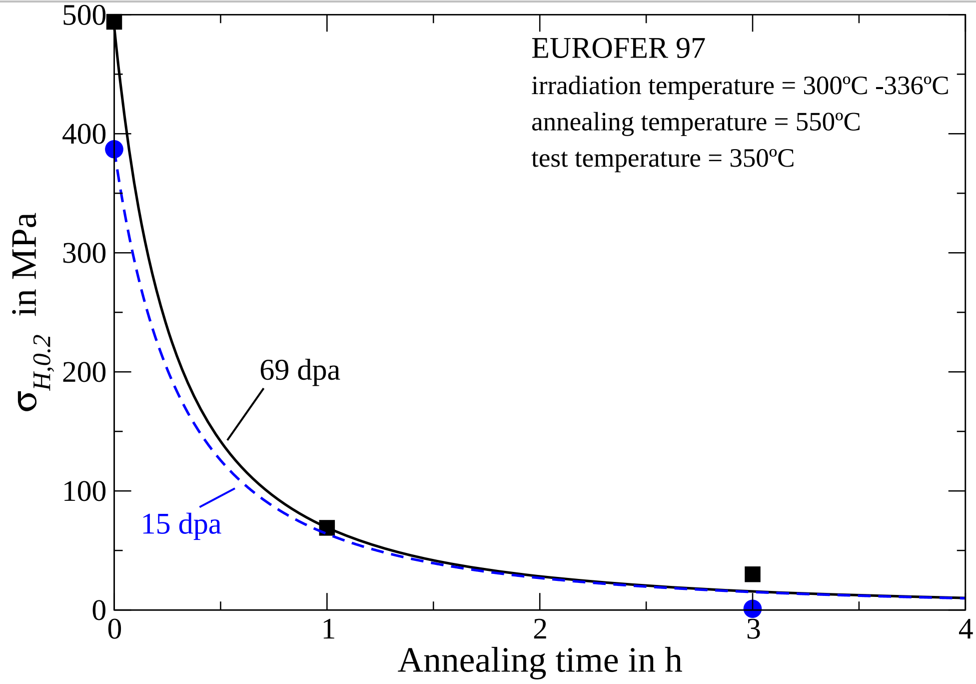

Figure 4: Influence of annealing time on irradiation induced hardening; comparison between experimental data (makers) and model description (solid lines) [14].

5.2 Use of the model for LCF lifetime prediction

The model parameters determined so far for EUROFER 97 allow the prediction of its coupled deformation damage behavior in the unirradiated state under arbitrary loading at any temperature between room temperature and 550°C whereas the dependence of the model parameters on temperature is covered by determining the parameter values at certain temperatures and interpolating linearly between these temperatures. For EUROFER 97 in the irradiated states predictions can be done for its behavior at least at the temperatures at which the tensile and LCF tests of the ARBOR I and II programs are performed.

Evaluating the LCF tests of the ARBOR I and II programs the tests performed on EUROFER 97 in the reference unirradiated state at 330°C (≈ irradiation temperature) are first considered. These tests were conducted using SSTT (small specimen test technology) specimens with the same size and geometry the irradiated LCF specimens have [16]. In Fig. 5 the LCF lifetimes as they observed experimentally are plotted versus the strain range and compared with those predicted by the model for the tests on SSTT specimens at 330°C as well as on standard LCF specimens at room temperature (RT) and 450°C. While the predicted lifetimes as expected lie between those observed experimentally from and predicted as well for the LCF tests performed at RT and 450°C on standard LCF specimens, the lifetimes of the SSTT specimens at 330°C unexpectedly are even lower than those observed on standard LCF specimens at 450°C. Apparently, SSTT fatigue specimens yield significantly lower (up to 5 times) lifetimes than standard fatigue specimens which however can not be straightforward considered by the model. This size effect might have many causes. One of them is that the surface quality of the SSTT specimens, which actually shall be scaled in comparison to that of the standard specimen, might not be sufficient or hard to produce for the size selected. One possibility to take into account this size effect by the model is to readjust the model parameters particularly those of the damage evolution equation (Eq. 12) by fitting the model to the behavior observed on SSTT specimens what by the way was done once as few experimental data and less knowledge about the model parameters values at low temperatures were available demonstrating the prediction capability of the model [14]. However, this would imply the assumption of a dependence of the model parameters on the size which is not in terms of the approach within the model has been developed. Other options for considering the size effects are currently investigated whereas the need therefore is not clear yet (see below).

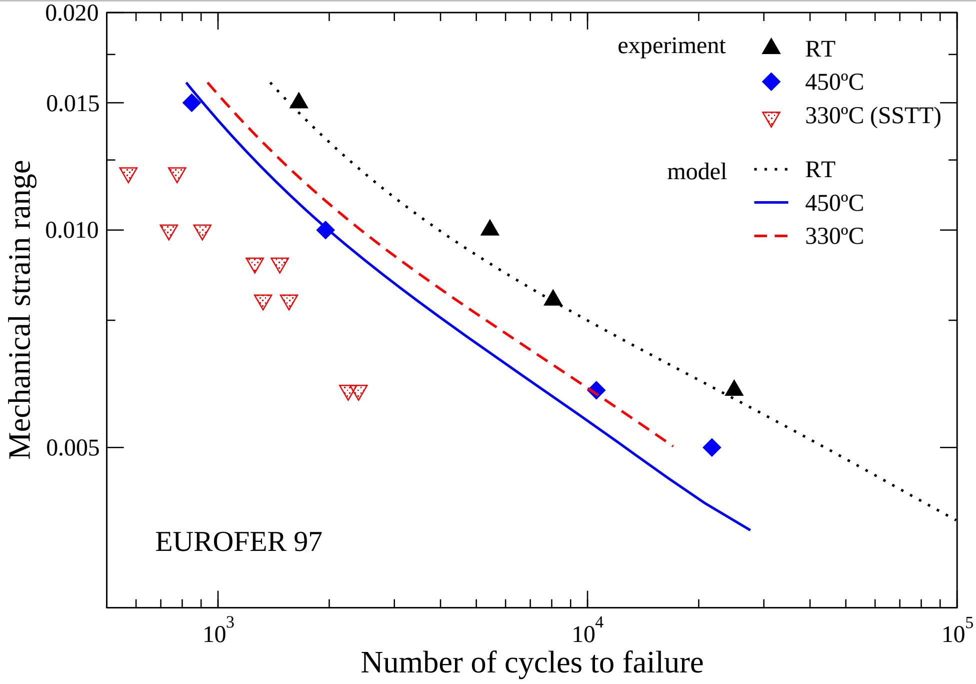

Figure 5: Low cycle fatigue behavior of unirradiated EUROFER 97; comparison between experimental data (markers) and model prediction (solid lines) as well as comparison between data from tests on standard specimens (filled markers) and those from tests on small size specimens (SSTT) [15].

With the same values of the model parameters, i.e. without any adjustments for taking the size effect mentioned above into account, the model application is proceeded considering the LCF tests performed on irradiated EUROFER 97. Figure 6 shows a comparison between the model predictions and the experimental results. For discussion the model predictions for the fatigue lifetimes of the unirradiated EUROFER 97 at the same temperature are illustrated in addition. It can be recognized that at high strain ranges a decrease of the fatigue lifetime due to irradiation is expected by the model. This is mainly attributed to the higher stresses resulting from the irradiation induced hardening which are that high that the lower inelastic strain within a cycle and thus its reduced influence on the fatigue damage are compensated. With lower strain ranges the inelastic strain within a cycle is strongly reduced and even vanishes resulting in fatigue lifetimes higher than those of the un-irradiated material (see Figure 6) which tends to infinity due to the lack of damage evolution (cf. Eq. 12). In addition, it can be recognized in Figure 6 that the predicted influence of irradiation on the LCF lifetime saturates toward higher irradiation doses (the calculated curves for irradiation doses higher than 31 dpa lie very close to each other, see Figure 6). The experimental LCF lifetimes verify the model predictions whereas except for one data point only the experimentally observed lifetimes are within a range of factor of two in comparison to those predicted by the model (see Figure 6). Since the LCF tests are performed on irradiated SSTT specimens, this is not necessary expected because the size effect mentioned above. However, the good model predictions allow for the speculation that the specimen size effect on the fatigue lifetime becomes insignificant after irradiation. An explanation for this could be that due to irradiation the capability for inelastic deformation is strongly reduced and microscopically limited to shear bands fewer than those activated in the unirradiated material. Consequently, possible surface flaws are not early activated due to the lack of slip activities in their areas and, hence, can not reduce the lifetime as they may do in the unirradiated specimen.

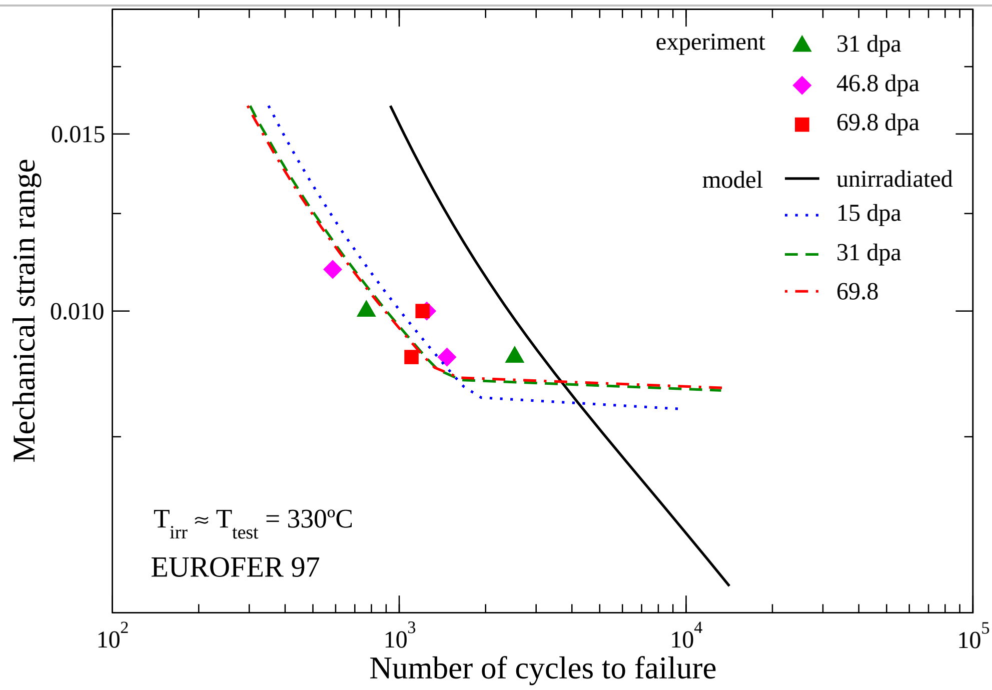

Figure 6: Influence of high dose irradiation on the low cycle fatigue of EUROFER 97; comparison between experimental data (makers) and model prediction (lines) [15].

6 Conclusions

The physically based model developed for the description of irradiation induced hardening does not only allow for the determination of hardening due to neutron irradiation, but also of its alteration under inelastic deformation and high temperature dwell conditions. Its coupling with the model describing the deformation and damage behavior of RAFM steels in the unirradiated state provides a powerful tool for the prediction of the constitutive behavior of RAFM steels during and after neutron irradiation under low cycle fatigue conditions. When applying the model to EUROFER°97 and F82H mod after neutron irradiation, fairly good results could be obtained determining the model parameters at 300 - 350°C and predicting the deformation behavior observed in post irradiation examinations.

Applying the model to predict the low cycle fatigue behavior of irradiated EUROFER 97 the negative influence of irradiation on the fatigue lifetime at high strain ranges could be fairly well reproduced. At low strain ranges the model predicts higher fatigue lifetimes and even endurance for irradiated EUROFER 97 which however is not yet verified by the experiments. The good results obtained so far give hope that the specimen size effect on the fatigue lifetime as observed on unirradiated EUROFER 97 becomes insignificant after irradiation and consequently does not need to be considered by the model in further applications on post irradiation low cycle fatigue experiments.

7 Acknowledgment

This work, supported by the European Communities under the contract of Association between EURATOM and Forschungszentrum Karlsruhe, was carried out within the framework of the European Fusion Development Agreement. The views and opinions expressed herein do not necessarily reflect those of the European Commission.

8 IP reporting

All the works provided under the present task were according to the current state-of-the art. No foreground IPR has been produced under this task. All information from involved external companies and sub-contractors is open and available, and no confidentiality or license agreement was signed. No invention or software development has to be declared.

9 References

[1] A. Hishinuma, A. Kohyama, R. L. Klueh, D. S. Gelles, W. Dietz and K. Ehrlich, Journal of Nuclear Materials, 258-263 (1998) 193-204.

[2] R.L. Klueh, Current Opinion in Solid State and Materials Science, 8 (2004) 239-250.

[3] E. Gaganidze, H.-C. Schneider, B. Dafferner and J. Aktaa, Journal of Nuclear Materials, 367-370 (2007) 81-85.

[4] C. Petersen, A. Povstyanko, V. Prokhorov, A. Fedoseev, O. Makarov and B. Dafferner, Journal of Nuclear Materials, 367-370 (2007) 544-549.

[5] J. Aktaa and R. Schmitt, Fusion Engineering and Design, 81 (2006) 2221-2231.

[6] J. L. Bement, R. G. Hoagland and F. A. Smidt, Fracture, ed. Liebowitz, Academic Press, 1971, vol. III, pp. 535-587.

[7] J. Marian, B.D. Wirth, R. Schäublin, G. R. Odette, J. Manuel Perlado, Journal of Nuclear Materials, 323 (2003) 181-191.

[8] R. L. Klueh, D. S. Gelles, S. Jitsukawa, A. Kimura, G. R. Odette, B. van der Schaaf, M. Victoria, Journal of Nuclear Materials, 307-311 (2002) 455-465.

[9] M. J. Makin and F. J. Minter, Acta Met. 8 (1960) 691-699.

[10] B. Mastel, H. E. Kissinger, J. J. Laidler and T. K. Bierlein, Journal of Applied Physics, 34 (1963) 3637-3638.

[11] J. Aktaa and C. Petersen, Engineering Fracture Mechanics 76 (2009) 1474-1484.

[12] E. Lucon et al., Fusion Engineering and Design, 81 (2006) 917-923.

[13] A. Alamo, J.L. Bertin, V.K. Shamardin and P. Wident, Journal of Nuclear Materials 367-370 (2007) 54-59.

[14] J. Aktaa and C. Petersen, Journal of Nuclear Materials 389 (2009) 432-435.

[15] J. Aktaa and C. Petersen, ICFRM 14, 2009.

[16] C. Petersen, V. Shamardin, A. Fedoseev, G. Shimansky, V. Efimov, and J. Rensman, Journal of Nuclear Materials 307-311 (2002) 1655-1659.